Evaluation of the permeation kinetics of formamide in porcine articular cartilage

Rachael Dong[a], Shannon Clark[b], Leila Laouar[a], Luke Heinrichs[a], Kezhou Wu[a,c], Nadr M. Jomha[a], Janet A.W. Elliott[b,d*]

[a] Department of Surgery, University of Alberta, Edmonton, Alberta, Canada

[b] Department of Chemical and Materials Engineering, University of Alberta, Edmonton, Alberta, Canada

[c] Department of Orthopedic Surgery, First Affiliated Hospital, Shantou University Medical College, Shantou, Guangdong, China

[d] Department of Laboratory Medicine and Pathology, University of Alberta, Edmonton, Alberta, Canada

* Corresponding author: janet.elliott@ualberta.ca

Abstract

Cryopreservation of articular cartilage will increase tissue availability for osteochondral allografting and improve clinical outcomes. However, successful cryopreservation of articular cartilage requires the precise determination of cryoprotectant permeation kinetics to develop effective vitrification protocols. To date, permeation kinetics of the cryoprotectant formamide in articular cartilage have not been sufficiently explored. The objective of this study was to determine the permeation kinetics of formamide into porcine articular cartilage for application in vitrification. The permeation of dimethyl sulfoxide was first measured to validate existing methods from our previously published literature. Osteochondral dowels from dissected porcine femoral condyles were incubated in 6.5 M dimethyl sulfoxide for a designated treatment time (1 s, 1 min, 2 min, 5 min, 10 min, 15 min, 30 min, 60 min, 120 min, 180 min, 24 h) at 22 °C (N = 3). Methods were then repeated with 6.5 M formamide at one of three temperatures: 4 °C, 22 °C, 37 °C (N = 3). Following incubation, cryoprotectant efflux into a wash solution occurred, and osmolality was measured from each equilibrated wash solution. Concentrations of effluxed cryoprotectant were calculated and diffusion coefficients were determined using an analytical solution to Fick's law for axial and radial diffusion in combination with a least squares approach. The activation energy

of formamide was determined from the Arrhenius equation. The diffusion coefficient (2.7–3.3 × 10^{-10} m^2/s depending on temperature) and activation energy (0.9 ± 0.6 kcal/mol) for formamide permeation in porcine articular cartilage were established. The determined permeation kinetics of formamide will facilitate its precise use in future articular cartilage vitrification protocols.

Keywords: Permeation kinetics, Formamide, Diffusion coefficient, Activation energy, Cryoprotectant, Cryopreservation, Vitrification, Articular Cartilage, Pig

1. Introduction

Articular cartilage is a connective tissue that functions to minimize friction during movement and is subjected to high levels of biomechanical stress [8,18,29]. Due to the avascular nature of articular cartilage, it has limited capacity for chondrocyte recovery following tissue injury [8,18,29]. Additionally, articular cartilage defects are considered a major risk factor in developing osteoarthritis [6,12,20]. Osteochondral allografting has shown to be effective in treating large, focal articular cartilage defects [7,9,11]. Unfortunately, osteochondral allografting procedures are often delayed by mandatory infectious diseases testing, regulatory clearance, problems with size and contour matching, and limited tissue availability [19,33]. The current method of hypothermically storing articular cartilage at 4 °C leads to significantly decreased cell viability after 28 days, limiting its utility [3,35]. Alternatively, cryopreservation of articular cartilage offers a comprehensive solution to these challenges and a path to improved clinical outcomes. As such, it remains critical to develop effective articular cartilage preservation techniques.

Vitrification is a promising cryopreservation technique [5,16,17,22] that utilizes high concentrations of cryoprotectants, also called cryoprotective agents (CPAs), to achieve a

49 suspended animation of chondrocytes at ultralow temperatures [5,22,38]. A major challenge that
50 arises from high CPA concentrations is cytotoxicity [2,13,24,36]. To ameliorate this toxicity while
51 maximizing permeation to ensure adequate cryoprotective effects, the precise determination of
52 CPA permeation kinetics is required.

53 Previous studies by our group have described the permeation kinetics of four common
54 CPAs into porcine articular cartilage: dimethyl sulfoxide (Me_2SO), ethylene glycol, glycerol, and
55 propylene glycol [23,31]. However, the permeation kinetics of formamide, another common CPA,
56 have remained unstudied.

57 Formamide is a relatively small amide that is considered highly toxic [2,4,24–26].
58 Although formamide alone cannot be used for vitrification as its molecules tend to self-associate
59 rather than associate with water [4,15,21,28], there is evidence that use of formamide in
60 combination with other CPAs results in cytotoxicity reduction [2,14,24,34]. Fahy demonstrated
61 that when used in combination with Me_2SO, formamide displayed diminished toxic effects [14].
62 Inclusion of formamide in future vitrification protocols may be valuable, particularly in multi-CPA
63 protocols. The objective of the study described herein was to determine the temperature-dependent
64 permeation kinetics of formamide at a concentration appropriate for vitrification, using our
65 previously established methods [1,23,31].
66

67 **2. Materials and methods**

68 *2.1 Experimental materials and methods*

69 Porcine stifle joints from sexually mature pigs prepared for meat consumption were
70 retrieved from Delton Sausage House & Deli (Edmonton, AB) within 24 hours after slaughter, and

were transported to the laboratory in a cooler. No animals were specifically sacrificed for this study. The use of animal tissue for research was approved by the Research Ethics Office at the University of Alberta. Distal femoral condyles were isolated following joint dissection; both medial and lateral condyles were used. Osteochondral dowels (10 mm diameter full thickness articular cartilage on subchondral bone base) were prepared using a custom hand-held coring device. Between two and four osteochondral dowels were gathered from the weight-bearing portion of each condyle. The subchondral bone base of each osteochondral dowel was then removed using a scalpel, and the remaining articular cartilage discs 1.1–2.9 mm thick were stored at 4 °C in 1 × phosphate-buffered saline (1 × PBS; Gibco).

Experimental methods were initially verified using Me_2SO mixed in isotonic 1 × PBS to compare with results previously published by our group [23,31]. For the 6.5 M Me_2SO treatment group, each articular cartilage disc was assigned to one of eleven incubation time treatments (1 s, 1 min, 2 min, 5 min, 10 min, 15 min, 30 min, 60 min, 120 min, 180 min, 24 h) at 22 °C. The negative control group consisted of an articular cartilage disc incubated in 1 × PBS only. Trials were performed three times. A total of 36 articular cartilage discs were used.

Identical methods were applied to formamide mixed in isotonic 1 × PBS for novel determination of formamide permeation kinetics. For the 6.5 M formamide treatment group, each articular cartilage disc was assigned to one of eleven CPA incubation time treatments (1 s, 1 min, 2 min, 5 min, 10 min, 15 min, 30 min, 60 min, 120 min, 180 min, 24 h) at one of three temperatures (4 °C, 22 °C, 37 °C). Negative control groups consisted of articular cartilage discs incubated in 1 × PBS only (at respective temperatures). Trials were performed three times at each temperature. A total of 108 articular cartilage discs were used.

93 Articular cartilage discs were removed from the PBS and excess fluid was removed from
94 cartilage surfaces using Kimwipes™ Delicate Task Wipes (Kimberly-Clark). Articular cartilage
95 discs were weighed (W_1) using weighing boats and a balance (AB54-S, Mettler Toledo).
96 Immediately after weighing, articular cartilage discs were individually placed in 6-well plates with
97 low evaporation lids (Fisher) containing 5 mL of CPA; the discs were fully submerged for the
98 assigned durations and each trial was run in duplicate. Sample plates were made airtight with
99 Parafilm™ to prevent evaporation. Plates were pre-cooled, and incubation was conducted in a
100 temperature-controlled laboratory cold room for the 4 °C treatment group. Incubation was
101 conducted in a laboratory room (maintained at 22 °C) for the 22 °C treatment group. Plates were
102 pre-warmed, and incubation was conducted in a temperature-controlled biological incubator for
103 the 37 °C treatment group.

104 Following incubation, articular cartilage discs were removed from the CPA-containing
105 wells. Excess fluid was again removed from cartilage surfaces using Kimwipes™ and a second
106 weight (W_2) was recorded. Articular cartilage discs were individually placed in 6-well plates with
107 low evaporation lids (Fisher) containing 4 mL of 1 × PBS wash solution. Regardless of
108 temperature treatment, all sample plates were sealed with Parafilm™, covered with aluminium
109 foil, and placed in dark conditions at 22 °C for 24 h to permit CPA efflux from the discs. Articular
110 cartilage discs were removed post-24 h and set aside for cartilage thickness measurements.
111 Resulting wash solutions were thoroughly mixed using a pipettor. From each equilibrated solution,
112 1 mL was collected into a 1.5 mL microcentrifuge tube. This solution was mixed and 50 µL was
113 collected for osmolality measurement using a micro-osmometer.

114 Articular cartilage disc thicknesses were measured using a digital caliper. In accordance
115 with previously published methodology by our group, thicknesses were measured at three different

locations for each disc, with the distal tips of the caliper jaws clamped at the centre of the circular articular cartilage discs [37]. Values were averaged for each disc.

The experimental methods are summarized in Figure 1.

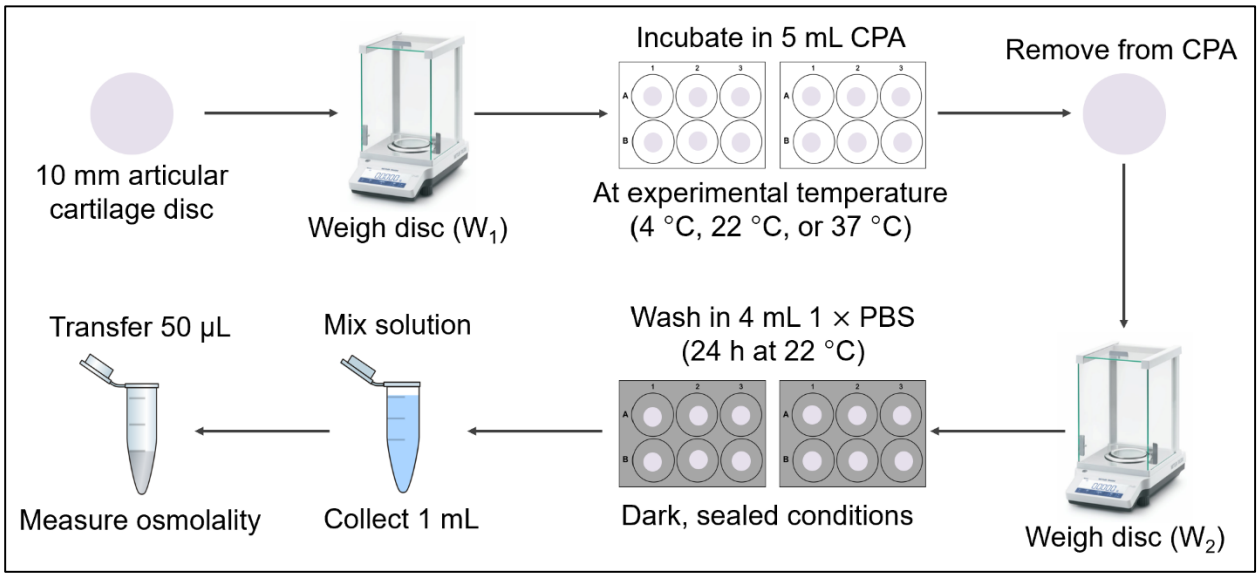

Figure 1. Summary of experimental methods. Osteochondral dowels were weighed and incubated in 5 mL of CPA at experimental temperature (4 °C, 22 °C, or 37 °C) for assigned durations. Following incubation, osteochondral dowels were removed from CPA, weighed a second time, and placed in 4 mL 1 × PBS for 24 h under dark, sealed conditions. Equilibrated wash solutions were mixed and osmolality indicating effluxed CPA was measured. Measured values were used to calculate average CPA concentrations in the tissue after each incubation duration.

2.2 Calculation methods

The average CPA concentration in the articular cartilage was calculated using a similar method to that previously used in our group [1,23]. The number of moles of CPA that permeated the cartilage, n_{CPA}, was calculated from the change in osmolality of the 1 × PBS solution as

$$n_{CPA}(\text{mol}) = \frac{[\pi_s - \pi_{one\ second}](\text{mosm/kg}) \times V_{sol}\ (\text{mL}) \times \rho_{water}(\text{g/mL})}{1000(\text{mosm/osm}) \times 1000(\text{g/kg})} \quad (1)$$

133 where π_s is the measured osmolality of the solution after CPA efflux, $\pi_{one\ second}$ is the osmolality
134 of the solution after CPA efflux for a one second CPA immersion trial, V_{sol} is the total volume of
135 the solution, and ρ_{water} is the density of water at 22 °C (0.99777 g/mL) [23]. The osmolality
136 $\pi_{one\ second}$ was subtracted from π_s instead of the osmolality of the original 1 × PBS solution to
137 account for CPA present on the surface of the cartilage that did not permeate. The total volume of
138 the solution includes the space within the articular cartilage that is capable of holding solution in
139 addition to the 4 mL volume of 1 × PBS. It was calculated as

140 $$V_{sol}(\mathrm{mL}) = 4\ \mathrm{mL} + 0.776 \times \frac{[\pi \times R^2(\mathrm{mm}^2) \times a\ (\mathrm{mm})]}{1000\ (\mathrm{mm}^3/\mathrm{mL})} \quad (2)$$

141 by assuming that each cartilage dowel is a perfect cylinder with a radius $R = 5$ mm and a unique
142 thickness a measured for each dowel (1.1–2.9 mm). A factor of 0.776 is applied as the fraction of
143 isotonic cartilage volume that is capable of holding the CPA solution [31]. The weight of the CPA,
144 W_{CPA}, was then calculated as

145 $$W_{CPA}(\mathrm{g}) = n_{CPA}(\mathrm{mol}) \times M_{CPA}(\mathrm{g/mol}) \quad (3)$$

146 where M_{CPA} is the molecular weight of the CPA. The volume of the CPA, V_{CPA}, was calculated as

147 $$V_{CPA}(\mathrm{mL}) = \frac{W_{CPA}(\mathrm{g})}{\rho_{CPA}(\mathrm{g/mL})} \quad (4)$$

148 where ρ_{CPA} is the pure density of the CPA at the appropriate temperature (Me_2SO at 22 °C (1.098
149 g/ML); formamide at 4, 22, and 37 °C (1.147, 1.132, and 1.119 g/mL)) [39]. The dry weight, W_{dry},
150 of each cartilage sample was calculated using

151 $$W_{dry}(\mathrm{g}) = W_1(\mathrm{g}) \times 0.224 \quad (5)$$

152 where 0.224 is the dry weight fraction of porcine articular cartilage [31]. Then, the volume of water
153 in the treated cartilage, V_{water}, could be determined by

$$V_{water}(\mathrm{mL}) = \frac{W_2(\mathrm{g}) - \left[W_{dry}(\mathrm{g}) + W_{CPA}(\mathrm{g})\right]}{\rho_{water}(\mathrm{g/mL})} \tag{6}$$

where ρ_{water} is the density of water at the appropriate temperature (0.999973, 0.99777, 0.99336 g/mL at 4, 22, and 37 °C, respectively) [23]. The average concentration of CPA in the cartilage, C_{CPA}, was then calculated as follows:

$$C_{CPA}(\mathrm{mol/L}) = \frac{n_{CPA}(\mathrm{mol}) \times 1000(\mathrm{mL/L})}{V_{CPA}(\mathrm{mL}) + V_{water}(\mathrm{mL})}. \tag{7}$$

Fick's law was used to model the diffusion of CPA into the articular cartilage dowel. The shape of each cartilage dowel was represented as a disc. Since the cartilage was removed from the bone, it was exposed to the CPA solution from the top, bottom, and sides. The surface area of the sides of the dowel is not negligible compared to the surface area of the top and bottom, so diffusion must be considered in both the axial and radial dimensions. The following analytical solution of Fick's law for 2D axial and radial diffusion into uniform discs was reported by Skelland [32]

$$\frac{\overline{C} - C^*}{C_0 - C^*} = \left[\frac{8}{\pi^2}\sum_{n=0}^{\infty}\frac{1}{(2n+1)^2}\exp\left(\frac{-D(2n+1)^2\pi^2 t}{4(a/2)^2}\right)\right] \times \left[\frac{4}{R^2}\sum_{n=1}^{\infty}\frac{1}{b_n^2}\exp(-Db_n^2 t)\right] \tag{8}$$

and was previously used by our group to calculate the diffusion coefficients for several CPAs in articular cartilage [1,23]. $\overline{C}$ (M) is the average concentration of CPA in the cartilage after time t (s), C_0 (M) is the initial average concentration, C^* (M) is the boundary condition concentration, a (m) is the thickness of the dowel, R (m) is the radius of the dowel, D (m^2/s) is the diffusion coefficient, and b_n (m^{-1}) is the nth root of the zero-order Bessel function of the first kind divided by the radius (i.e., $J_0(b_n R) = 0$). The initial concentration, C_0, was taken to be zero since no CPA was initially present in the cartilage. The boundary condition, C^*, was taken to be the concentration in the cartilage after 24 hours. The thickness, a, was taken to be the average thickness of the

articular cartilage discs used at each temperature (1.7, 1.8, and 1.5 mm for 4, 22, and 37 °C, respectively).

All computations were performed in MATLAB R2020a (Natick, MA). The roots of the zero-order Bessel function of the first kind were calculated using the function *besselzero* [27]. The infinite sums were computed by adding terms until the addition of the subsequent term did not change the total value of the sum based on MATLAB's default precision of 16 significant digits. The diffusion coefficient, D, was determined such that it minimized the sum of squared errors between the Fick's law predictions and the experimental data. This calculation was performed by summing the squared errors for values of D in the range 0.1–100 $\times 10^{-10}$ m^2/s and selecting the value with the lowest error. A precision of two significant figures was chosen, so the tested values of D were increased in 0.1 $\times 10^{-10}$ m^2/s increments. To verify that refining the test increment did not impact the results, the same process was repeated in increments of 0.01 $\times 10^{-10}$ m^2/s. The same results were obtained.

The temperature dependence of diffusion coefficients can be expressed by the Arrhenius equation as

$$D = A\exp\left(-\frac{E_a}{RT}\right) \tag{9}$$

where E_a is the activation energy (kcal/mol), A is the prefactor (m^2/s), T is the absolute temperature (K), and R is the universal gas constant (1.9872 $\times 10^{-3}$ kcal/(mol K)). The equation was linearized, and the activation energy and prefactor were found using linear regression.

3. Results

The results obtained in this study for the permeation of Me_2SO into articular cartilage at 22 °C are compared to those reported previously by our group [23] in Figure 2. The results of the present study agree with the previous results, which gives confidence in the experimental methods used. The same methods were applied to the formamide trials.

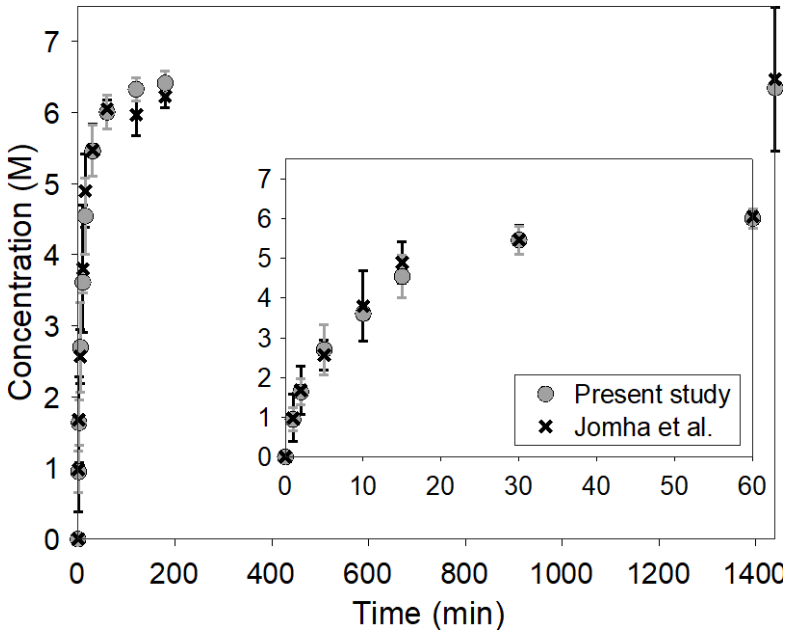

Figure 2. Comparison of the data obtained in the present study and the data reported previously by our group [23] for the permeation of 6.5 M Me_2SO into porcine articular cartilage at 22 °C. The inset shows the Me_2SO permeation during the first 60 min of exposure when the uptake is most rapid. The numerical values of the data in this figure are given in Table S1 in the Supplementary Material.

Figure 3 shows the concentration of formamide in articular cartilage during permeation at various temperatures. All three temperatures exhibit the same permeation pattern of a sharp increase in formamide concentration during the first 15 min of exposure followed by a gradual increase until 180 min and then eventual plateau. At 37 °C, the initial uptake of formamide is slightly steeper than at the lower temperatures of 4 and 22 °C. Table 1 lists the Fick's law diffusion coefficients for formamide that were determined in this work alongside previously determined

212 diffusion coefficients for other CPAs for the sake of comparison. The diffusion coefficient at 37
213 °C is lower than at 22 °C despite the figure showing faster permeation at 37 °C. This observation
214 can be explained by the fact that the articular cartilage discs used for the 37 °C trials were on
215 average thinner than those used at 22 °C (1.5 mm versus 1.8 mm) and by noting that the rate of
216 permeation depends both on the diffusion coefficient and on the thickness of articular cartilage
217 discs. The thicknesses were taken into account during fitting, which resulted in a lower diffusion
218 coefficient at 37 °C.
219

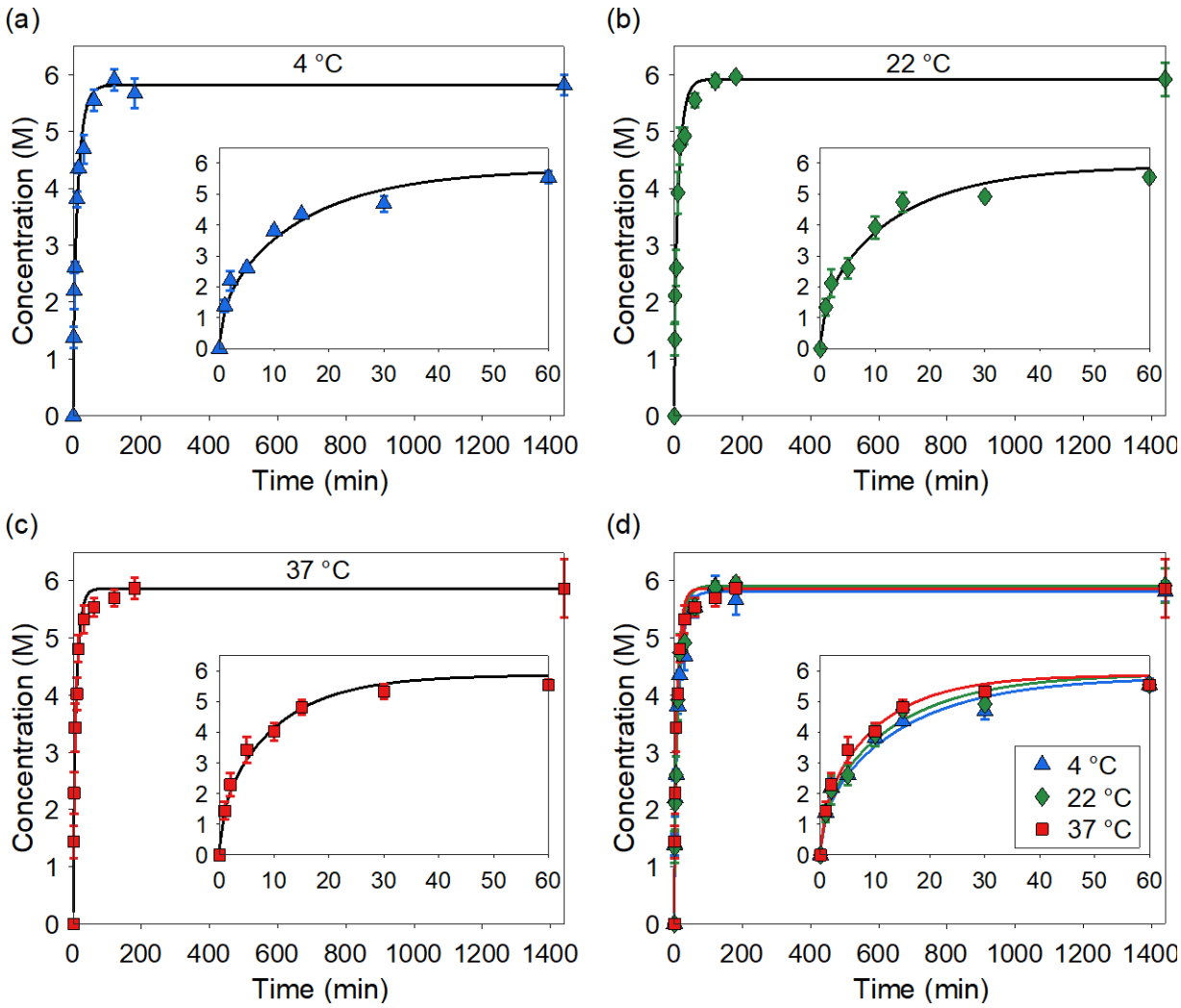

Figure 3. (a)–(c) Permeation of 6.5 M formamide into porcine articular cartilage at 4, 22, and 37 °C over 24 hours. The solid lines illustrate the Fick's law fit using the diffusion coefficient that minimized the sum of squared errors between the experimental data and the model. The insets show formamide permeation during the first 60 min of exposure when the uptake is most rapid. (d) Comparison of formamide permeation at different temperatures to illustrate the effect of temperature on permeation rate. The numerical values of the data in this figure are given in Table S1 in the Supplementary Material.

Table 1. Diffusion coefficients (m^2/s) for formamide (this work) and other CPAs (previous work) at three temperatures [1,23].

Temperature	4 °C	22 °C	37 °C
Formamide	$\mathbf{2.7 \times 10^{-10}}$	$\mathbf{3.3 \times 10^{-10}}$	$\mathbf{3.2 \times 10^{-10}}$
Me_2SO	2.6×10^{-10}	3.1×10^{-10}	5.7×10^{-10}
Ethylene glycol	2.0×10^{-10}	2.7×10^{-10}	4.2×10^{-10}
Glycerol	0.8×10^{-10}	1.8×10^{-10}	2.3×10^{-10}
Propylene glycol	1.0×10^{-10}	2.1×10^{-10}	3.6×10^{-10}

Figure 4 shows the Arrhenius plot illustrating the temperature dependence of formamide's diffusion coefficient. The activation energy for formamide with standard error was found to be $E_a = 0.9 \pm 0.6$ kcal/mol. The prefactor for formamide was found to be $A = 1.5079 \times 10^{-9}$ m^2/s.

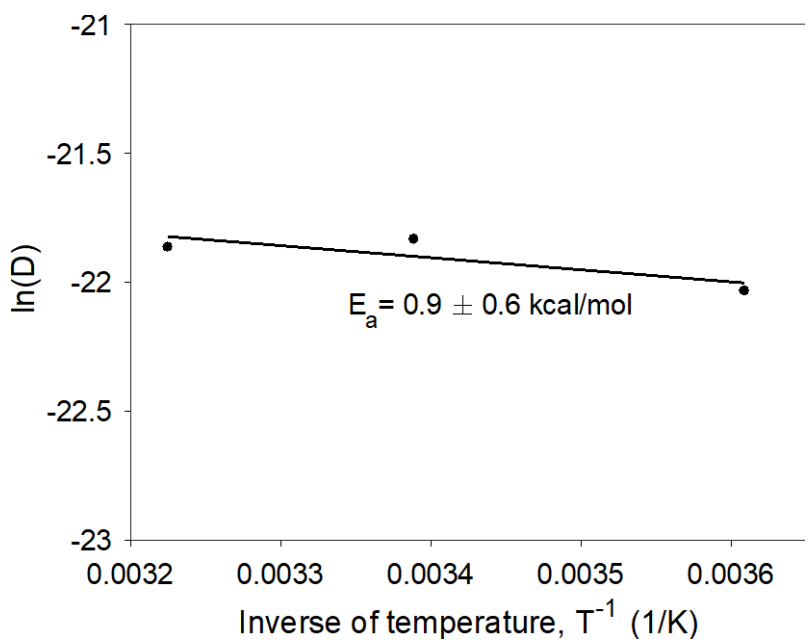

Figure 4. Arrhenius plot showing the temperature dependence of formamide's diffusion coefficient. Diffusion coefficients (D) were in units of m^2/s.

Figure 5 shows the normalized weights of the articular cartilage discs during formamide permeation at various temperatures. At all temperatures the weight initially drops upon exposure

to formamide but quickly returns to its original value after 1 min. After this point, the weight increases above its original value until reaching somewhat of a plateau. There appears to be no significant difference in the weight change during formamide loading at different temperatures. The numerical values of the weight data for formamide permeation shown in Figure 5 are given in Table S2 in the Supplementary Material along with the weight data for Me_2SO permeation.

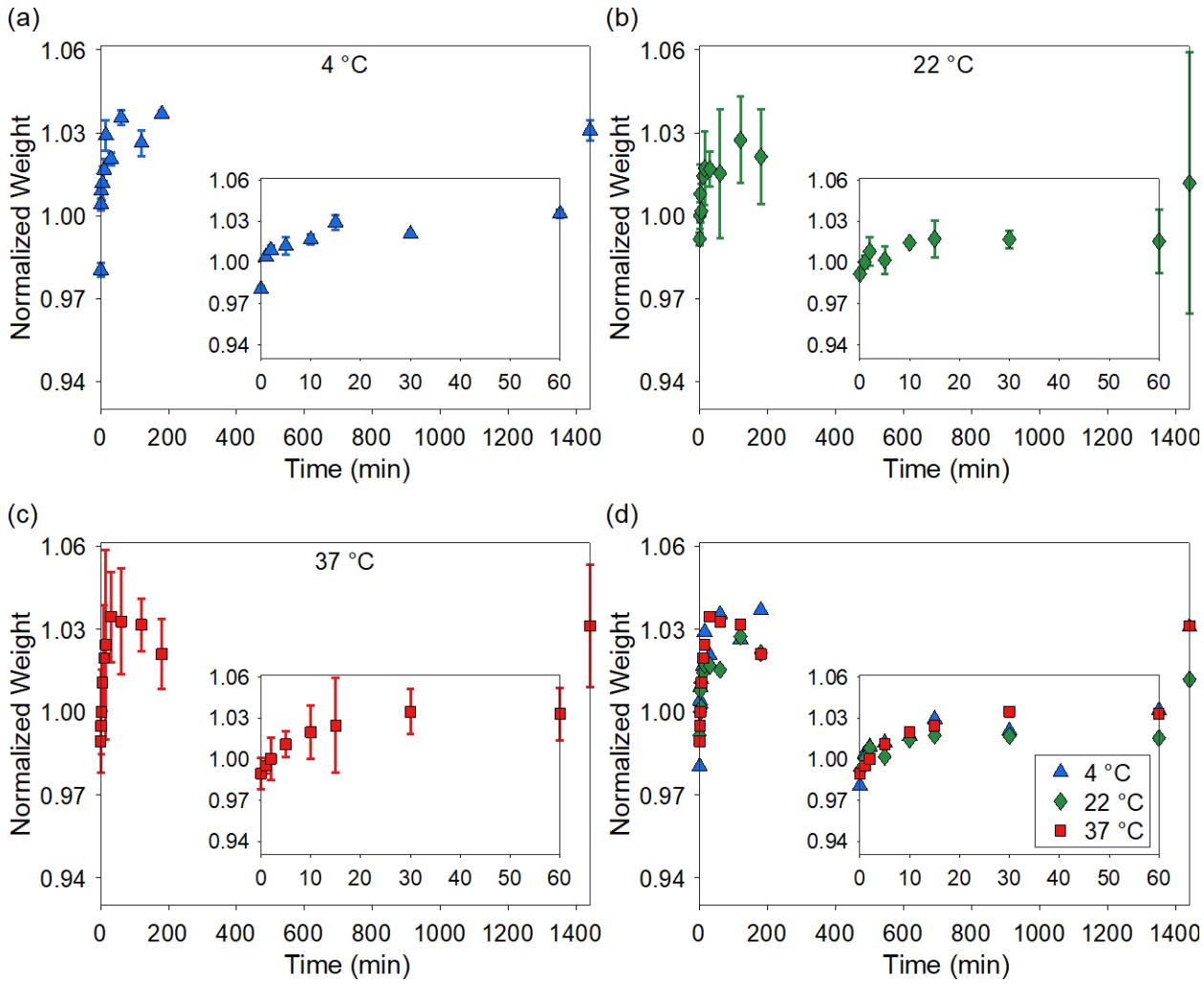

Figure 5. (a)–(c) Normalized weight (W_2/W_1) of the articular cartilage discs during permeation of 6.5 M formamide at 4, 22, and 37 °C over 24 hours. The inset shows the normalized weight during the first 60 min of exposure when the formamide uptake is most rapid. (d) Comparison of normalized weight during formamide permeation at different temperatures. Error bars are omitted from this panel to ensure readability. The numerical values of the data in this figure are given in Table S2 in the Supplementary Material.

Figure 6 presents a comparison between the concentrations of Me_2SO and formamide in articular cartilage over different exposure times at 22 °C. The diffusion coefficient for Me_2SO at 22 °C was found to be $D = 2.4 \times 10^{-10}$ m^2/s. Although both CPA solutions were 6.5 M, the final

concentration in the cartilage exposed to Me_2SO was greater than that of the cartilage exposed to formamide. We do not know the reason for this.

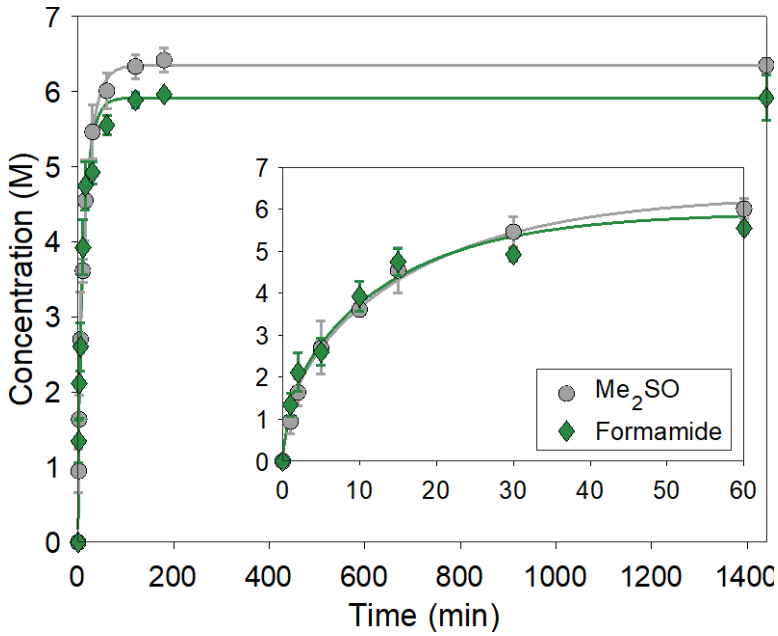

Figure 6. Comparison of the permeation of 6.5 M Me_2SO or 6.5 M formamide into porcine articular cartilage at 22 °C. The solid lines illustrate the Fick's law fit using the diffusion coefficient that minimized the sum of squared errors between the experimental data and the model. The inset shows Me_2SO and formamide permeation during the first 60 min of exposure when the uptake is most rapid.

4. Discussion & Conclusion

Use of formamide in combination with other CPAs may be conducive to optimization of vitrification protocols, particularly by reducing cytotoxicity [2,14,24]. By determining the precise permeation kinetics of formamide, we can incorporate these results into future mathematical modelling of combined CPA protocols. This mathematical modelling will allow for sufficient formamide exposure during vitrification while minimizing its toxic effects. Previous quantifications of CPA permeation kinetics have contributed to optimization of CPA loading time for the vitrification of articular cartilage by Shardt et al. [30], and to successful vitrification of intact human articular cartilage by Jomha et al. [22] and of both porcine and human articular cartilage cubes by Wu et al. [38].

The results of this study yield diffusion coefficients (2.7–3.3 $\times 10^{-10}$ m^2/s depending on temperature) and an activation energy (0.9 ± 0.6 kcal/mol) for formamide permeation in porcine articular cartilage. Diffusion coefficients for formamide permeation in porcine articular cartilage reported herein complement previous data collected by our group for the permeation kinetics of four other CPAs often used in current porcine articular cartilage vitrification protocols (Me_2SO, ethylene glycol, glycerol, propylene glycol) [23]. Secondary to this, the Me_2SO diffusion coefficient obtained in this work is slightly lower but still highly congruous with previous experiments (2.4×10^{-10} m^2/s (current) compared to 3.0– 3.1 $\times 10^{-10}$ m^2/s and 3.5×10^{-10} m^2/s (previous)) [1,23,31]. The discrepancy may be explained by the use of actual measured values for articular cartilage disc thicknesses in the calculations for this work, rather than the approximated 2 mm that was used in the previous study. Our Me_2SO diffusion coefficients are of the same order of magnitude as diffusion coefficients for human articular cartilage obtained under different conditions by Carsi et al. [10]. Due to the improved accuracy in articular cartilage disc thickness

measurement along with successful reproduction of previously published experimental methods, we have confidence in our results.

In addition to diffusion coefficients, the activation energy of formamide was also calculated ($E_a = 0.9 \pm 0.6$ kcal/mol). The activation energy of formamide is lower than that of other CPAs previously studied (Me_2SO: $E_a = 3.9 \pm 1.6$ kcal/mol, ethylene glycol: $E_a = 3.8 \pm 0.7$ kcal/mol, glycerol: $E_a = 5.6 \pm 1.2$ kcal/mol, and propylene glycol: $E_a = 6.63 \pm 0.04$ kcal/mol) [1,23], which indicates that the diffusion rate of formamide in porcine articular cartilage is less temperature-dependent. With a precise formamide activation energy, we will be able to predict permeation rates at all sub-zero temperatures involved in vitrification protocols.

A critical challenge in the vitrification of articular cartilage has been maximizing CPA permeation to achieve optimal cryoprotective effects, while minimizing cytotoxicity from the high concentrations of CPA required [2,14,24]. While previous studies have already accurately determined the permeation kinetics of four common CPAs (Me_2SO, ethylene glycol, glycerol, and propylene glycol) [23,31], this study provides comprehensive data on formamide temperature-dependent permeation kinetics, making it available for future mathematical modelling of vitrification protocols alongside the aforementioned CPAs. Given evidence that formamide interacts with other CPAs to reduce cytotoxicity (particularly Me_2SO) [2,14,24], formamide permeation kinetics will be a valuable tool for optimization of multi-CPA vitrification protocols moving forward.

Author contributions

Experiment designed by R. Dong, L. Laouar, K. Wu, N.M. Jomha and J.A.W. Elliott. Experiment and data acquisition performed by R. Dong, L. Laouar and L. Heinrichs. Data analysis and

mathematical simulations performed by S. Clark, R. Dong and J.A.W. Elliott. R. Dong and S. Clark wrote the first manuscript draft with guidance from J.A.W. Elliott, and all authors reviewed and revised the final manuscript for publication.

Conflicts of interest

N.M. Jomha and J.A.W. Elliott are co-inventors on the US (8,758,988) and Canada (2,788,202) patents for articular cartilage preservation: N.M. Jomha, L. E. McGann, J.A.W. Elliott, G. Law, F. Forbes, A. Abazari Torghabeh, B. Maghdoori, A. Weiss, University of Alberta, "Cryopreservation of articular cartilage".

Acknowledgements

This research was funded by the Edmonton Orthopaedic Research Committee. J.A.W. Elliott holds a Canada Research Chair in Thermodynamics. R. Dong received funding from the University of Alberta Faculty of Medicine and Dentistry through the Department of Surgery Summer Studentship, and the Edmonton Orthopaedic Research Committee. S. Clark received funding from the Natural Sciences and Engineering Research Council (NSERC) of Canada through the Undergraduate Student Research Award. K. Wu is funded by the Li Ka Shing Sino-Canadian Exchange Program between University of Alberta and Shantou University. We thank Delton Sausage House & Deli in Edmonton for providing us with porcine joints for this research project.

References

[1] A. Abazari, N.M. Jomha, G.K. Law, J.A.W. Elliott, L.E. McGann, Erratum to "Permeation of several cryoprotectants in porcine articular cartilage" [Cryobiology 58 (2009) 110–114], Cryobiology 59 (2009) 369.

[2] K.A. Almansoori, V. Prasad, J.F. Forbes, G.K. Law, L.E. McGann, J.A.W. Elliott, N.M. Jomha, Cryoprotective agent toxicity interactions in human articular chondrocytes, Cryobiology 64 (2012) 185–191.

[3] S.T. Ball, D. Amiel, S.K. Williams, W. Tontz, A.C. Chen, R.L. Sah, W.D. Bugbee, The Effects of Storage on Fresh Human Osteochondral Allografts, Clin. Orthop. Relat. Res. 418 (2004) 246–252.

[4] B.P. Best, Cryoprotectant Toxicity: Facts, Issues, and Questions, Rejuvenation Res. 18 (2015) 422–436.

[5] K.G.M. Brockbank, Z.Z. Chen, Y.C. Song, Vitrification of porcine articular cartilage, Cryobiology 60 (2010) 217–221.

[6] J.A. Buckwalter, Articular Cartilage: Injuries and Potential for Healing, J. Orthop. Sports Phys. Ther. 28 (1998) 192–202.

[7] W.D. Bugbee, A.L. Pallante-Kichura, S. Görtz, D. Amiel, R. Sah, Osteochondral allograft transplantation in cartilage repair: Graft storage paradigm, translational models, and clinical applications, J. Orthop. Res. 34 (2016) 31–38.

[8] C.B. Carballo, Y. Nakagawa, I. Sekiya, S.A. Rodeo, Basic Science of Articular Cartilage, Clin. Sports Med. 36 (2017) 413–425.

[9] F. de Caro, S. Bisicchia, A. Amendola, L. Ding, Large Fresh Osteochondral Allografts of the Knee: A Systematic Clinical and Basic Science Review of the Literature, Arthroscopy. 31 (2015) 757–765.

[10] B. Carsi, J.L. Lopez-Lacomba, J. Sanz, F. Marco, L. Lopez-Duran, Cryoprotectant permeation through human articular cartilage, Osteoarthr. Cartil. 12 (2004) 787–792.

[11] E.J. Cotter, C.P. Hannon, D.R. Christian, K.C. Wang, D.A. Lansdown, B.R. Waterman, R.M. Frank, B.J. Cole, Clinical Outcomes of Multifocal Osteochondral Allograft Transplantation of the Knee: An Analysis of Overlapping Grafts and Multifocal Lesions, Am. J. Sports Med. 46 (2018) 2884–2893.

[12] C. Ding, P. Garnero, F. Cicuttini, F. Scott, H. Cooley, G. Jones, Knee cartilage defects: association with early radiographic osteoarthritis, decreased cartilage volume, increased joint surface area and type II collagen breakdown, Osteoarthr. Cartil. 13 (2005) 198–205.

[13] H.Y. Elmoazzen, A. Poovadan, G.K. Law, J.A.W. Elliott, L.E. McGann, N.M. Jomha, Dimethyl sulfoxide toxicity kinetics in intact articular cartilage, Cell Tissue Bank 8 (2007) 125–133.

[14] G.M. Fahy, Cryoprotectant toxicity neutralization, Cryobiology. 60 (2010) S45–S53.

[15] G.M. Fahy, D.I. Levy, S.E. Ali, Some Emerging Principles Underlying the Physical Properties, Biological Actions, and Utility of Vitrification Solutions, Cryobiology 24 (1987) 196–213.

[16] G.M. Fahy, D.R. MacFarlane, C.A. Angell, H.T. Meryman, Vitrification as an Approach to Cryopreservation, Cryobiology 21 (1984) 407–426.

[17] G.M. Fahy, B. Wowk, J. Wu, J. Phan, C. Rasch, A. Chang, E. Zendejas, Cryopreservation of organs by vitrification: perspectives and recent advances, Cryobiology 48 (2004) 157–178.

[18] A.J.S. Fox, A. Bedi, S.A. Rodeo, The Basic Science of Articular Cartilage: Structure, Composition, and Function, Sports Health 1 (2009) 461–468.

[19] B. Goodfriend, A.A. Essilfie, I.A. Jones, C.T. Vangsness Jr., Fresh osteochondral grafting in the United States: the current status of tissue banking processing, Cell Tissue Bank 20 (2019) 331–337.

[20] E.B. Hunziker, Articular cartilage repair: basic science and clinical progress. A review of the current status and prospects, Osteoarthr. Cartil. 10 (2001) 432–463.

[21] J. Jadżyn, J. Świergiel, On similarity of hydrogen-bonded networks in liquid formamide and water as revealed in the static dielectric studies, Phys. Chem. Chem. Phys. 14 (2012) 3170–3175.

[22] N.M. Jomha, J.A.W. Elliott, G.K. Law, B. Maghdoori, J.F. Forbes, A. Abazari, A.B. Adesida, L. Laouar, X. Zhou, L.E. McGann, Vitrification of intact human articular cartilage, Biomaterials 33 (2012) 6061–6068.

[23] N.M. Jomha, G.K. Law, A. Abazari, K. Rekieh, J.A.W. Elliott, L.E. McGann, Permeation of several cryoprotectant agents into porcine articular cartilage, Cryobiology 58 (2009) 110–114.

[24] N.M. Jomha, A.D.H. Weiss, J. Fraser Forbes, G.K. Law, J.A.W. Elliott, L.E. McGann, Cryoprotectant agent toxicity in porcine articular chondrocytes, Cryobiology 61 (2010) 297–302.

[25] G.L. Kennedy, Formamide, in: P. Wexler (Ed.), Encyclopedia of Toxicology, 3rd ed., Elsevier, Wilmington, 2014: pp. 657–658.

[26] National Center for Biotechnology Information, PubChem Compound Summary for CID 713, Formamide. https://pubchem.ncbi.nlm.nih.gov/compound/Formamide. Accessed November 24, 2021.

[27] J. Nicholson, Bessel Zero Solver, MATLAB Central File Exchange, https://www.mathworks.com/matlabcentral/fileexchange/48403-bessel-zero-solver. Accessed June 12, 2020.

[28] R. Parthasarathi, V. Subramanian, N. Sathyamurthy, Hydrogen Bonding without Borders: An Atoms-in-Molecules Perspective, J. Phys. Chem. 110 (2006) 3349–3351.

[29] A.D. Pearle, R.F. Warren, S.A. Rodeo, Basic Science of Articular Cartilage and Osteoarthritis, Clin. Sports Med. 24 (2005) 1–12.

[30] N. Shardt, Z. Chen, S.C. Yuan, K. Wu, L. Laouar, N.M. Jomha, J.A.W. Elliott, Using engineering models to shorten cryoprotectant loading time for the vitrification of articular cartilage, Cryobiology 92 (2020) 180–188.

[31] R. Sharma, G.K. Law, K. Rekieh, A. Abazari, J.A.W. Elliott, L.E. McGann, N.M. Jomha, A novel method to measure cryoprotectant permeation into intact articular cartilage, Cryobiology 54 (2007) 196–203.

[32] A.H.P. Skelland, Diffusional Mass Transfer, Wiley-Interscience, New York, 1974.

[33] C.T. Vangsness Jr., I.A. Garcia, C.R. Mills, M.A. Kainer, M.R. Roberts, T.M. Moore, Allograft transplantation in the knee: tissue regulation, procurement, processing, and sterilization, Am. J. Sports Med. 31 (2003) 474–481.

423 [34] R.M. Warner, E. Ampo, D. Nelson, J.D. Benson, A. Eroglu, A.Z. Higgins, Rapid
424 quantification of multi-cryoprotectant toxicity using an automated liquid handling
425 method., Cryobiology 98 (2021) 219–232.
426 [35] R.J. Williams 3rd, J.C. Dreese, C.-T. Chen, Chondrocyte survival and material properties of
427 hypothermically stored cartilage: an evaluation of tissue used for osteochondral allograft
428 transplantation, Am. J. Sports Med. 32 (2004) 132–139.
429 [36] K. Wu, L. Laouar, R. Dong, J.A.W. Elliott, N.M. Jomha, Evaluation of five additives to
430 mitigate toxicity of cryoprotective agents on porcine chondrocytes, Cryobiology 88
431 (2019) 98–105.
432 [37] K. Wu, L. Laouar, N. Shardt, J.A.W. Elliott, N.M. Jomha, Osmometric Measurements of
433 Cryoprotective Agent Permeation into Tissues, in: W.F. Wolkers, H. Oldenhof (Eds.),
434 Cryopreservation and Freeze-Drying Protocols, Springer, New York, 2021: pp. 303–315.
435 [38] K. Wu, N. Shardt, L. Laouar, J.A.W. Elliott, N.M. Jomha, Vitrification of particulated
436 articular cartilage via calculated protocols, NPJ Regen. Med. 6 (2021) 15.
437 [39] C.L. Yaws, Yaws, Liquid densities - organic compounds, in: Electronic Edition Yaws'
438 Thermophysical Properties of Chemicals and Hydrocarbons, 2010.
439

Supplementary Information for "Evaluation of the permeation kinetics of formamide in porcine articular cartilage"

Rachael Dong[a], Shannon Clark[b], Leila Laouar[a], Luke Heinrichs[a], Kezhou Wu[a,c], Nadr M. Jomha[a], Janet A.W. Elliott[b,d*]

[a] Department of Surgery, University of Alberta, Edmonton, Alberta, Canada

[b] Department of Chemical and Materials Engineering, University of Alberta, Edmonton, Alberta, Canada

[c] Department of Orthopedic Surgery, First Affiliated Hospital, Shantou University Medical College, Shantou, Guangdong, China

[d] Department of Laboratory Medicine and Pathology, University of Alberta, Edmonton, Alberta, Canada

* Corresponding author: janet.elliott@ualberta.ca

The following tables contain the numerical values of data in the figures in the main text. In addition, the weight data for Me_2SO permeation are given only in the Supplementary Material and not in the main text.

Table S1. Concentration of CPA in porcine articular cartilage ± the standard deviation at each temperature and time of exposure to 6.5 M CPA.

CPA	Me_2SO	Formamide		
Temperature	22 °C	4 °C	22 °C	37 °C
1 s	0	0	0	0
1 min	0.95 ± 0.29 M	1.38 ± 0.19 M	1.34 ± 0.28 M	1.44 ± 0.28 M
2 min	1.64 ± 0.32 M	2.20 ± 0.31 M	2.11 ± 0.46 M	2.29 ± 0.37 M
5 min	2.70 ± 0.63 M	2.62 ± 0.09 M	2.60 ± 0.32 M	3.43 ± 0.42 M
10 min	3.61 ± 0.16 M	3.81 ± 0.14 M	3.92 ± 0.36 M	4.02 ± 0.29 M
15 min	4.55 ± 0.54 M	4.35 ± 0.08 M	4.74 ± 0.32 M	4.81 ± 0.24 M
30 min	5.46 ± 0.36 M	4.69 ± 0.25 M	4.92 ± 0.15 M	5.33 ± 0.24 M
60 min	6.01 ± 0.24 M	5.55 ± 0.19 M	5.55 ± 0.13 M	5.54 ± 0.17 M
120 min	6.33 ± 0.16 M	5.91 ± 0.19 M	5.88 ± 0.11 M	5.70 ± 0.14 M
180 min	6.42 ± 0.16 M	5.66 ± 0.26 M	5.96 ± 0.03 M	5.87 ± 0.19 M
24 h	6.35 ± 0.09 M	5.81 ± 0.18 M	5.91 ± 0.30 M	5.87 ± 0.51 M

Table S2. Normalized weight (W_2/W_1) of porcine articular discs ± the standard deviation at each temperature and time of exposure to 6.5 M CPA.

CPA	Me_2SO	Formamide		
Temperature	22 °C	4 °C	22 °C	37 °C
1 s	0.960 ± 0.010	0.980 ± 0.003	0.992 ± 0.002	0.989 ± 0.011
1 min	0.931 ± 0.017	1.004 ± 0.002	1.000 ± 0.005	0.995 ± 0.006
2 min	0.907 ± 0.011	1.009 ± 0.003	1.008 ± 0.011	1.000 ± 0.015
5 min	0.900 ± 0.010	1.012 ± 0.006	1.002 ± 0.010	1.011 ± 0.009
10 min	0.889 ± 0.025	1.017 ± 0.004	1.014 ± 0.001	1.020 ± 0.019
15 min	0.900 ± 0.011	1.029 ± 0.006	1.017 ± 0.013	1.025 ± 0.034
30 min	0.914 ± 0.045	1.021 ± 0.002	1.017 ± 0.006	1.035 ± 0.016
60 min	0.998 ± 0.034	1.036 ± 0.003	1.015 ± 0.023	1.033 ± 0.019
120 min	1.031 ± 0.022	1.026 ± 0.005	1.027 ± 0.016	1.032 ± 0.010
180 min	1.045 ± 0.008	1.037 ± 0.001	1.021 ± 0.017	1.021 ± 0.013
24 h	1.053 ± 0.004	1.031 ± 0.004	1.012 ± 0.047	1.031 ± 0.022